Core−Corona Structure of Cubic Silsesquioxane-Poly(Ethylene Oxide) in Aqueous Solution: Fluorescence, Light Scattering, and TEM Studies

K. Yi Mya,[†,§] Xu Li,[†,§] Ling Chen,[†] Xiping Ni,[†] Jun Li,[†,‡] and Chaobin He*[,†]

Institute of Materials Research and Engineering, 3 Research Link, Singapore 117602, Republic of Singapore and Division of Bioengineering, Faculty of Engineering, National University of Singapore, Singapore 117576, Republic of Singapore

Received: January 17, 2005; In Final Form: March 21, 2005

Well-defined amphiphilic cubic silsesquioxane-poly(ethylene oxide) (CSSQ-PEO) was prepared from octakis (dimethylsiloxy)octasilsesquioxane ($Q_8M_8^H$) and allyl-PEO through a hydrosilylation reaction. The structure of CSSQ-PEO was characterized by nuclear magnetic resonance (NMR), Fourier transform infrared spectroscopy (FTIR), and gel permeation chromatography (GPC). The amphiphilic properties and aggregation process of CSSQ-PEO in aqueous solution were investigated by fluorescence, dynamic and static light scattering (DLS and SLS), and transmission electron microscopy (TEM). The critical aggregation concentration (CAC) determined by fluorescence measurements was found to be 0.28 mg/mL. Combinations of DLS, SLS, and TEM studies showed the existence of core−corona micelle with hydrophobic CSSQ as the core and hydrophilic PEO as the corona in aqueous solution. The observation of two size distribution peaks from DLS measurements revealed the coexistence of small amounts of unassociated unimolecular micelles (∼10% of the scattered intensity) together with micellar aggregates when the CSSQ-PEO concentration was ≤2 mg/mL. The hydrodynamic radii (R_h) of unassociated unimolecular micelle and micellar aggregates were found to be 26 and 79 nm, respectively. A large R_g/R_h ratio (1.46) and the extremely small value of average chain density (4×10^{-4} g/cm^3) indicate the small hydrophobic CSSQ core was surrounded by the extended PEO coronae. The aggregation number (N_{agg}) of CSSQ-PEO in aqueous solution was found to be 38 ± 2 from SLS and 31−40 from TEM, respectively. The long PEO segments act as a spacer between the spherical aggregates, which facilitate the formation of a network-like structure at high concentration.

Introduction

Polyhedral oligomeric silsesquioxanes (POSS) have attained much interest in the past few years because of their well-defined nanostructure. Various types of POSS have been used as building blocks for precisely defined nanostructured functional materials[1−4] with improved thermal, mechanical, and optoelectronic properties.[5−8] The cubic structure of POSS, cubic silsesquioxane (CSSQ), has a nanosized inorganic core containing silica and eight organic functional groups on the silica surface with the diameter between 0.7 and 1.5 nm.[9−12] Although CSSQ have many potential applications in performance materials and biomedical fields, the problem encountered is its poor solubility in water. To achieve good solubility in water, hydrophilic groups are required to modify the structure of CSSQ. Because poly(ethylene oxide) (PEO) is a highly water-soluble polymer with remarkable properties, such as biocompatibility and nontoxicity, the incorporating of PEO onto CSSQ is of special interest in biotechnological applications.

Kim and Mather[13] reported the synthesis and characterization of amphiphilic telechelics PEG end-capped with CSSQ. The modification to the crystallization behavior of PEG was observed in the presence of monosubstituted CSSQ macromer because of the bulkiness of CSSQ groups with respect to crystalline lamellae dimensions. Different thermal and morphological properties were observed by controlling the balance of the hydrophilic PEG and the hydrophobic CSSQ macromer. The synthesis and thermal properties of oligomeric poly(ethylene oxide)-functionalized silsesquioxanes were reported by Maitra and Wunder.[14] Their studies showed how the thermal behavior of oligomeric PEO was influenced by the silica surface of CSSQ. Because of interfacial effects, the mobility of the PEO chain is reduced as observed by an increase in the glass-transition temperature (T_g) and suppression in crystallization compared to linear materials. Knischka et al.[15] reported the synthesis and the characterization of monosubstituted CSSQ, 1-(1,ω-propylenemethoxy)oligo (ethylene oxide)-3,4,7,9,11, 13,15-heptahydridopentacyclo octasiloxane. It was found that the self-organization of the amphiphiles in aqueous solution leads to micellar and vesicular structures that can be cross-linked to form liposome-like silica particles at elevated pH. These materials, therefore, are beneficial when applied as low-temperature solvents in lithium ion batteries with enhanced ion conductivity.

The properties of aggregates formed by associative polymers in aqueous solutions are of much interest not only in industry but also in fundamental research.[16] To our knowledge, although the synthesis and characterization of different types of monosubstituted CSSQ with PEO have been previously reported,[13−15] the aqueous solution properties and aggregation behavior of the amphiphilic multiarm CSSQ-PEO have received less attention. It is of interest, therefore, to study the properties and the aggregation behavior of amphiphilic multiarm CSSQ-PEO in aqueous solution.

* Author to whom correspondence should be addressed. E-mail: cb-he@imre.a-star.edu.sg.
† Institute of Materials Research and Engineering.
‡ National University of Singapore.
§ Equal contribution came from first author and second author.

10.1021/jp050287s CCC: $30.25
Published on Web 04/16/2005

Light scattering is a well-established method to determine several parameters, such as the diffusion coefficient (D), hydrodynamic radius (R_h), root-mean-square z-average radius of gyration ($\langle R_g^2 \rangle_z^{1/2}$) (normally written as R_g), weight average molecular weight (M_w), second virial coefficient (A_2), and the aggregation phenomena of macromolecules in solution. Lee and co-workers[17] recently reported the physical and viscoelastic properties of CSSQ-grafted hybrid copolymers of styrene and vinyl-diphenylphosphine oxide (PSP) by dynamic light scattering (DLS) and rheological measurements. It was observed that the hydrodynamic size of CSSQ-grafted copolymers in dilute solution slightly increased by the increment of CSSQ content and the linear viscoelastic response of CSSQ grafted copolymers changed from a viscoelastic liquidlike behavior to a gellike behavior at high CSSQ content attributable to intrachain interactions. Light scattering is probably the most convenient technique to study the actual shapes of macromolecules and to investigate the polymer−solvent interactions and intra- and interpolymer interactions in dilute solution.[18] Therefore, we report, for the first time, the physical properties and the aggregation behavior of amphiphilic multiarm CSSQ-PEO in aqueous solution. In this study, water-soluble PEO modified with a CSSQ macromer was prepared using octakis (dimethylsiloxy) octasilsesquioxane ($Q_8M_8^H$) and high-molecular-weight PEO. The amphiphilic properties and aggregation process of CSSQ-PEO in aqueous solution were carried out by fluorescence, dynamic and static light scattering (DLS and SLS), and transmission electron microscopy (TEM).

Experimental Section

Materials. Monomethyl end-capped poly(ethylene oxide) (M-PEO) with number average molecular weight of 2000 was purchased from Sigma-Aldrich and used as received. Allyl bromide (Aldrich) was distilled before use. A 10 wt % aqueous solution of methylammonium hydroxide (Aldrich), dimethylchlorosilane (Aldrich), and tetraethoxysilane (Aldrich) were used for the synthesis of CSSQ, namely, octakis (dimethylsiloxy) octasilsesquioxane ($Q_8M_8^H$) without further purification. Toluene was dried with sodium metal under nitrogen atmosphere. Platinum divinyltetramethyl disiloxane Pt(dvs) catalyst was obtained from Aldrich Co. and diluted to 2 mM solution in anhydrous toluene.

Synthesis of CSSQ-PEO. The allyl-terminated monomethyl PEO (allyl-PEO) was synthesized through the reaction of the hydroxyl end group of M-PEO with an excess amount of allyl bromide following the literature procedure.[19] $Q_8M_8^H$ was prepared according to the literature.[20,21] The CSSQ-PEO was synthesized by a hydrosilylation reaction as shown in Scheme 1. $Q_8M_8^H$ (0.50 g, 0.49 mmol) and 9.80 g (4.90 mmol) of allyl-PEO were dissolved into freshly dried toluene (∼50 mL) in a two-necked round-bottomed flask equipped with a Teflon-coated magnetic stirrer bar. Pt(dvs) catalyst (∼3 mL) was introduced into the flask after the complete dissolution of $Q_8M_8^H$ and allyl-PEO in toluene. The mixture was then stirred for 20 h at 85 °C under an argon atmosphere. The final product was isolated and purified by repeated fractionation in an anhydrous ether and methanol mixture and monitored by gel permeation chromatography (GPC) until the peak corresponding to allyl-PEO disappeared.

Characterization and Techniques. *^1H NMR.* ^{1}H NMR spectra for CSSQ and CSSQ-PEO in deuterated chloroform ($CDCl_3$) without tetramethylsilane (TMS) were obtained using a Bruker DRX 400 MHz NMR spectrometer. (a) CSSQ (δ, ppm): 0.25 [Si(CH_3)$_2$CH$_2$−], 4.72 [Si(CH$_3$)$_2$$H$]. (b) CSSQ-PEO ($\delta$, ppm): 0.16 [Si($CH_3$)$_2CH_2$−], 0.63 (Si$CH_2CH_2CH_2$O), 1.29 (SiCH$_2$$CH_2CH_2$O), 1.75 (SiCH$_2CH_2$$CH_2$O), 3.40 (−O$CH_3$), 3.65 (−$CH_2$$CH_2$O−).

SCHEME 1: Synthesis Route of CSSQ-PEO

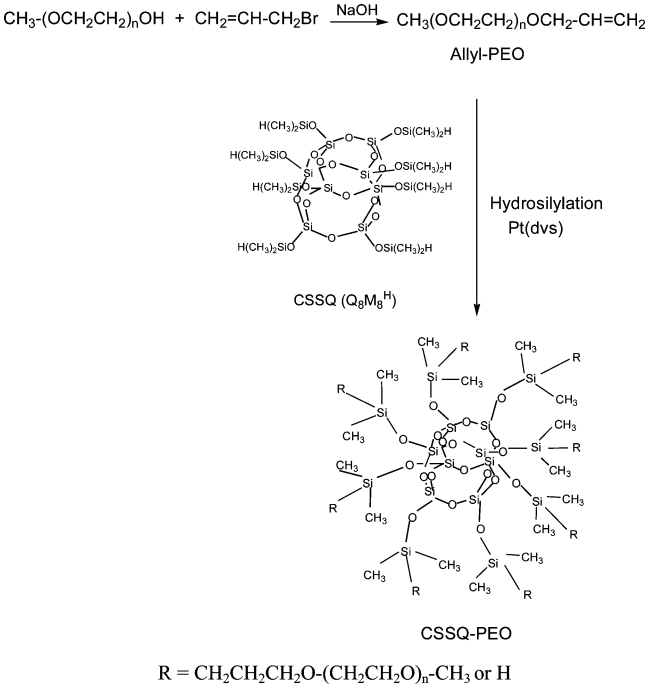

Fourier Transform Infrared Spectroscopy (FTIR). FTIR spectra were obtained using a FTIR Spectrum 2000 Spectrometer (Perkin Elmer Instruments, Inc.). The spectra were recorded with 32 scans, signal averaged with a resolution of 2 cm^{-1}. The solid samples were prepared by mixing with potassium bromide (KBr) and compressing the mixtures to a pellet. FTIR spectrum (cm^{-1}): 1120 (υ(Si−O−Si), δ(C−H)); 960 (δ(Si−CH$_3$), δ(C−O)); and 840 (δ(Si−CH$_2$), υ(C−O)).

Gel Permeation Chromatography (GPC). GPC data was recorded with a Shimadzu SCL-10A and LC-8A system equipped with two Phenogel 5μ 50- and 1000-Å columns in series and a Shimadzu RID-10A refractive index detector. The system was calibrated with monodisperse poly(ethylene glycol) standards and tetrahydrofuran (THF) was used as the eluent at a flow rate of 0.30 mL/min.

Refractive Index Increment (dn/dc). The dn/dc is an essential parameter to determine the absolute molecular weight of a polymer by static light scattering. Therefore, the refractive index of CSSQ-PEO aqueous solutions at different concentrations (0.1−0.5 mg/mL) was measured by using a Brookhaven differential refractometer at a wavelength of 620 nm to determine the value of dn/dc. Prior to measurement, the instrument was standardized with potassium chloride (KCl) in aqueous solution. It was found that the dn/dc of CSSQ-PEO solution is 0.147 mL/g at 25 °C.

Dynamic Light Scattering (DLS). The DLS study was performed using a Brookhaven (BI-200 SM) light scattering instrument. The light source was a 35-mW He−Ne laser emitting vertically polarized light of 632.8 nm wavelength. The sample cells were mounted in a temperature-controlled, refractive index matched bath filled with decahydronaphthalene (decalin). In the DLS measurements, the intensity correlation function was measured at 25 °C with a maximum number of 256 channels using a BI-9000AT digital autocorrelator. The calibration of the spectrometer was carried out using a polystyrene standard solution with a size of 97 ± 3.2 nm. DLS

measures the intensity−intensity autocorrelation function, $G^{(2)}(\tau)$, which is related to the electric field autocorrelation function, $G^{(1)}(\tau)$, by means of the Siegert relation[22]

$$|G^{(2)}(\tau)| = B[1 + \beta|G^{(1)}(\tau)|^2] \quad (1)$$

where B is the baseline and β is the spatial coherence factor, depending on the collection efficiency of the detector. The electric field autocorrelation function, $G^{(1)}(\tau)$, is characterized by a distribution function of the decay rate (Γ) from

$$|G^{(1)}(\tau)| = \int G(\Gamma) \exp(-\Gamma\tau)\mathrm{d}\Gamma \quad (2)$$

with $\Gamma = Dq^2$. Γ is the decay rate and q is the scattering vector that depends on the scattering angle θ ($q = 4\pi n/\lambda_0 \sin \theta/2$), where n is the refractive index of the suspending liquid and λ_0 is the laser wavelength in vacuo. For spherical particles, the decay time ($\tau = 1/\Gamma$) is related to the translational diffusion coefficient (D_t), providing that the internal relaxation modes are negligible. The hydrodynamic radius (R_h) was determined by the Stokes−Einstein relationship $D_t = k_B T/(6\pi\eta R_h)$, where k_B, η, and T are the Boltzmann constant, the viscosity of solvent, and the absolute temperature, respectively.

Static Light Scattering (SLS). The intensity measurements were carried out at different scattering angles (30−120°) to evaluate the radius of gyration (R_g), second virial coefficient (A_2), and molecular weight (M_w) of CSSQ-PEO in aqueous solution. By measuring the optical constant (K) and the excess Rayleigh ratio (ΔR_θ) at infinite dilution, the M_w, A_2, and R_g can be evaluated using the Zimm−Debye equation

$$\frac{Kc}{\Delta R_\theta} = \left[\frac{1 + q^2 R_g^2}{3}\right]\left[\frac{1}{M_w} + 2A_2 c\right] \quad (3)$$

where K is the optical constant, which depends on the refractive index increment of the polymer solution ($K = 4\pi^2 n^2 (\mathrm{d}n/\mathrm{d}c)^2/N_A\lambda^4$). Here, $\mathrm{d}n/\mathrm{d}c$ is the refractive index increment of the CSSQ-PEO aqueous solution, N_A is Avogadro's number, and ΔR_θ is the excess Rayleigh ratio [$\Delta R_\theta = R_\theta$(solution) − R_θ(solvent)], respectively. The extrapolation of $Kc/\Delta Rq$ to $q \rightarrow 0$ and $c \rightarrow 0$ leads to M_w, and the slopes of angle and concentration dependence give rise to A_2 and R_g. Prior to both DLS and SLS measurements, the deionized water was filtered through 0.2 μm Millipore membrane filters (Whatman) to remove dust particles. The CSSQ-PEO solutions were centrifuged at 8000 rpm for 30 min and then filtered with 0.22 μm Millipore filters directly into the light scattering cell.

Fluorescence Measurements. The excitation measurements were carried out between 290 and 360 nm with an emission wavelength of 373 nm at 25 °C with pyrene as a fluorescent probe using a Shimadzu RF-5301 PC spectrofluorophotometer. A series of CSSQ-PEO solutions with concentrations ranging from 0.001 to 5 mg/mL were prepared by diluting a CSSQ-PEO stock solution with deionized water. A solution of pyrene dissolved in methanol was transferred to a number of cylindrical vials, and methanol was then evaporated under nitrogen before an equal amount of CSSQ-PEO solutions was added to give a final pyrene concentration of 6.0×10^{-7} M. The concentration of the pyrene was fixed and the CSSQ-PEO concentration was varied throughout the measurements.

Transmission Electron Microscopy (TEM). TEM micrographs were obtained using a Philips CM300 FEGTEM operating at an accelerating voltage of 300 kV. A drop of CSSQ-PEO aqueous solution was cast onto a 200-mesh carbon-coated copper grid. The samples were dried at room temperature prior to measurement.

Results and Discussion

The octafunctional cubic silsesquioxane ($Q_8M_8^H$) was prepared according to the Hasegawa method.[20] The CSSQ-PEO was synthesized by a two-step reaction as shown in Scheme 1. The allyl terminated PEO was obtained by an allylation reaction of monomethyl PEO with excess amount of allyl bromide. In the second step, the hydrophilic segments of allyl PEO are attached to CSSQ ($Q_8M_8^H$) by hydrosilylation leading to the formation of amphiphilic CSSQ-PEO. Figure 1 shows the ^{1}H NMR spectra of CSSQ ($Q_8M_8^H$) (Figure 1a) and CSSQ-PEO (Figure 1b), in which all proton signals belonging to both PEO and CSSQ are observed. The formation of CSSQ-PEO is confirmed by the disappearance of the Si−H signal at 4.72 ppm, accompanied by the appearance of methylene protons signal at 0.63 ppm, although the signal is very small, as indicated in Figure 1b. The number of PEO chains attached to the CSSQ core can be determined from the ratio between the integrals of peaks for the methylene group at 0.63 ppm and the methyl group at 0.16 ppm. ^{1}H NMR resonance integration shows that six PEO chains attached to each CSSQ on average. It is difficult to obtain the complete substitution of CSSQ because of the steric hindrance of high molecular weight PEO.

The FTIR spectrum of CSSQ-PEO (Figure 2) clearly shows the symmetric stretching of the Si−O−Si peak at 1120 cm^{-1}, corresponding to the silsesquioxane cage structure. The characteristic peaks of aliphatic C−H stretching are observed at 2920 and 2960 cm^{-1}. The stretching and bending peaks for the Si−CH_3 group are also observed at 1250 and 960 cm^{-1}, respectively. A small peak appeared at 2150 cm^{-1} and is due to the retained Si−H group, which is in agreement with the incomplete substitution of CSSQ observed by ^{1}H NMR. The absorption bands at 960 and 840 cm^{-1} are the overlay of the Si−C groups and the characteristic peaks of the crystalline phase of PEO.[23,24] All of the characteristic absorption bands for CSSQ-PEO agree well with the results obtained from the ^{1}H NMR spectra.

GPC analysis was performed to determine the molecular weight and molecular weight distribution of CSSQ-PEO. Figure 3 shows the GPC results for allyl-PEO, CSSQ ($Q_8M_8^H$), and CSSQ-PEO chromatograms. All three chromatographs show unimodal distributions. The GPC spectra for allyl-PEO and CSSQ ($Q_8M_8^H$) appeared at longer retention times, with number average molecular weights (M_n) of 2140 and 870, respectively, compared to that of CSSQ-PEO. The smaller measured value of M_n for CSSQ relative to the theoretical calculated M_n of 1016 is due to the use of linear poly(ethylene glycol) in calibration. The GPC chromatogram of CSSQ-PEO reveals the increase in molecular weight obtained by the covalent linkage of PEO with CSSQ. The M_n, M_w, and the molecular weight distribution (M_w/M_n) of CSSQ-PEO are determined to be 11 650, 12 950, and 1.11, respectively, indicating approximately five PEO chains were attached to the CSSQ core. This result is lower than the theoretically expected value for CSSQ, with six PEO chains estimated from the ^{1}H NMR result. It is not surprising that CSSQ-PEO has a spherical micellar structure while the standard PEG is a linear chain. Nevertheless, a relatively narrow and unimodal distribution ($M_w/M_n = 1.11$) of CSSQ-PEO confirms the successful synthesis of CSSQ-PEO as shown in Scheme 1.

The aggregation behavior of CSSQ-PEO in aqueous solution was investigated by fluorescence measurement using pyrene as a probe. This method has been widely used to determine the aggregation process of amphiphilic polymers in aqueous solu-

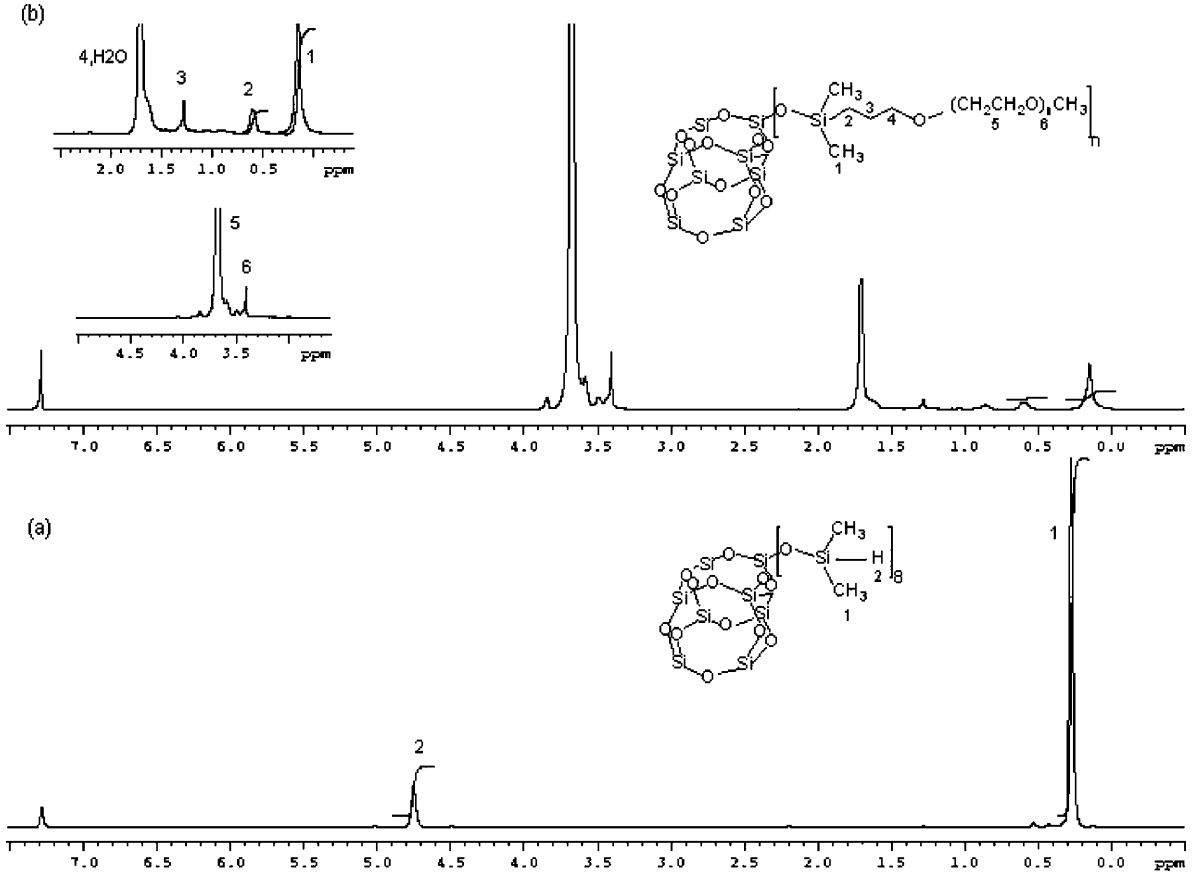

Figure 1. ^{1}H NMR spectra for (a, bottom) CSSQ ($Q_8M_8^H$) and (b, top) CSSQ-PEO in $CDCl_3$ at room temperature.

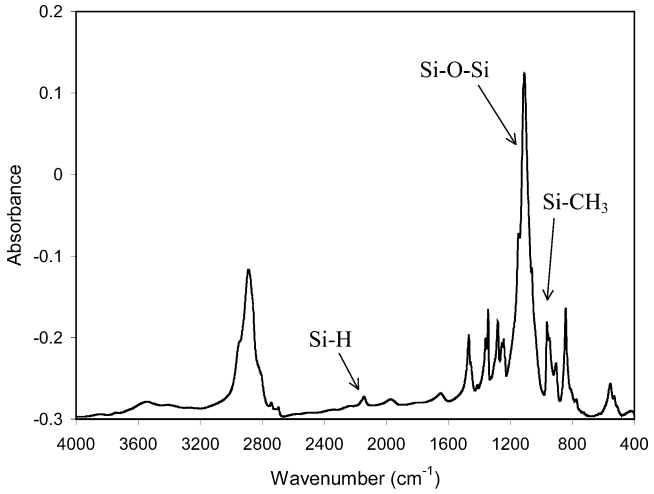

Figure 2. FTIR spectrum of CSSQ-PEO.

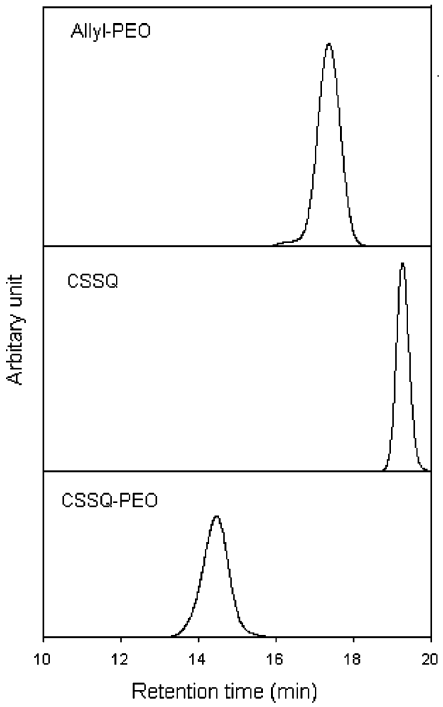

Figure 3. GPC chromatograms for Allyl-PEO (M_n = 2140, M_w/M_n = 1.02), CSSQ (M_n = 870, M_w/M_n = 1.00), and CSSQ-PEO (M_n = 11,650, M_w/M_n = 1.11).

tion.[25] Figure 4 shows the fluorescence excitation spectra for CSSQ-PEO at different concentrations in a fixed pyrene concentration of 6.0×10^{-7} M. The excitation peak at 334 nm shifts to 337 nm when pyrene is surrounded by the hydrophobic environment. At low concentrations, CSSQ hydrophobic domains are so small that pyrene molecules are mainly solubilized in the aqueous phase. When aggregation occurs by the addition of CSSQ-PEO, large hydrophobic domains are formed within the aggregates, and the pyrene preferentially penetrates into the hydrophobic core. This leads to the shift of the excitation band to higher wavelengths, as indicated in Figure 4. The difference in the excitation spectra can be characterized by the intensity ratio of I_{337}/I_{334}. Figure 5 shows the intensity ratio (I_{337}/I_{334}) of the pyrene monomer as a function of the logarithm of the CSSQ-PEO concentration. The critical aggregation concentration (CAC) is identified by the inflection point in I_{337}/I_{334} versus concentration plot, which is determined to be 0.28 mg/mL.

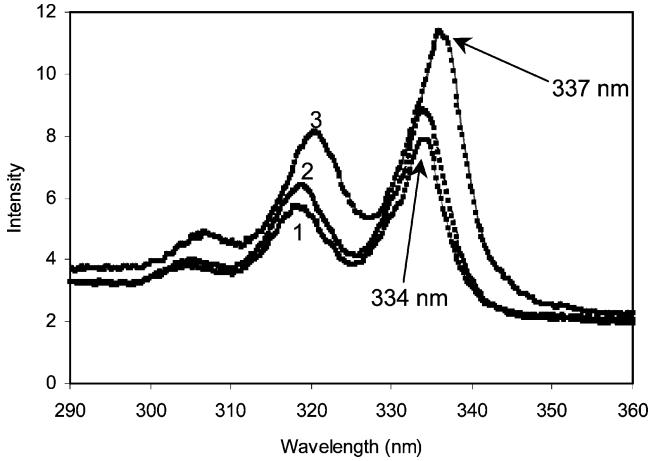

Figure 4. Fluorescence excitation spectra for CSSQ-PEO at different concentrations *in a fixed pyrene concentration* (6.0×10^{-7} M). (1) 0.05 mg/mL; (2) 0.25 mg/mL; (3) 5 mg/mL.

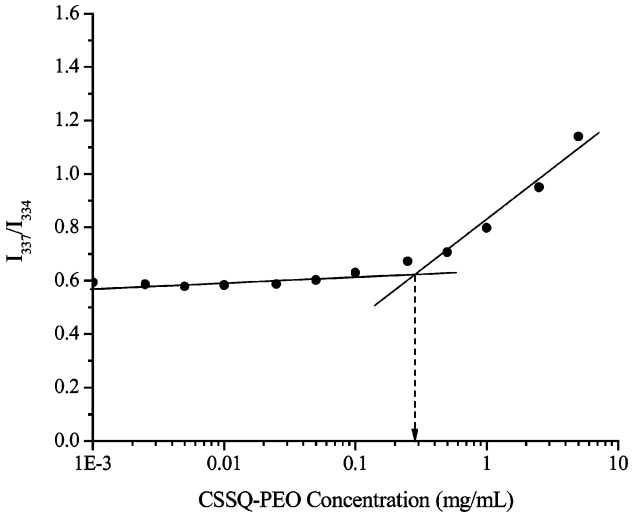

Figure 5. Variation of the intensity ratio (I_{337}/I_{334}) as a function of CSSQ-PEO concentration. The dotted arrow shows the CAC value.

Dynamic and static light scattering studies were also carried out to investigate the hydrodynamic properties and aggregation behavior of CSSQ-PEO in aqueous solution. The CAC value determined by fluorescence measurements is so low (0.28 mg/mL) that insufficient scattering intensity was encountered in the light scattering studies in this concentration range. Therefore, the concentrations of CSSQ-PEO in the light scattering studies were above the CAC (0.5−5 mg/mL). In this case the determination of unimolecular micelles in aqueous solution without aggregation is extremely difficult. Figure 6 shows the size distribution function of CSSQ-PEO at different concentrations measured at 90°. Two size distribution peaks are observed at concentrations ≤2 mg/mL, although the scattered intensity of the first peak is very weak (∼10%). The small peak represents the unassociated unimolecular micelle with R_h = ∼26 nm and the dominant peaks attributed to the scattering from the large particles attributable to the aggregation of CSSQ-PEO. The aggregation peak is observed, even at a concentration of 0.5 mg/mL, indicating that the CAC of CSSQ-PEO is lower than 0.5 mg/mL, which is in agreement with the fluorescence measurements (CAC = 0.28 mg/mL). While the size of unassociated unimolecular micelles remains fairly constant, the size of the micellar aggregates shifts to larger values with increasing concentration of CSSQ-PEO. The broad distribution at a concentration of 5 mg/mL is a result of the interconnections

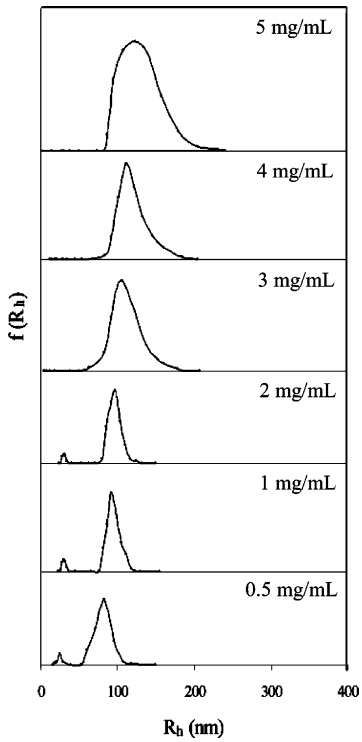

Figure 6. Concentration dependence of hydrodynamic radius distribution functions of CSSQ-PEO. (Bottom to top: 0.5, 1.0, 2.0, 3.0, 4.0, and 5.0 mg/mL).

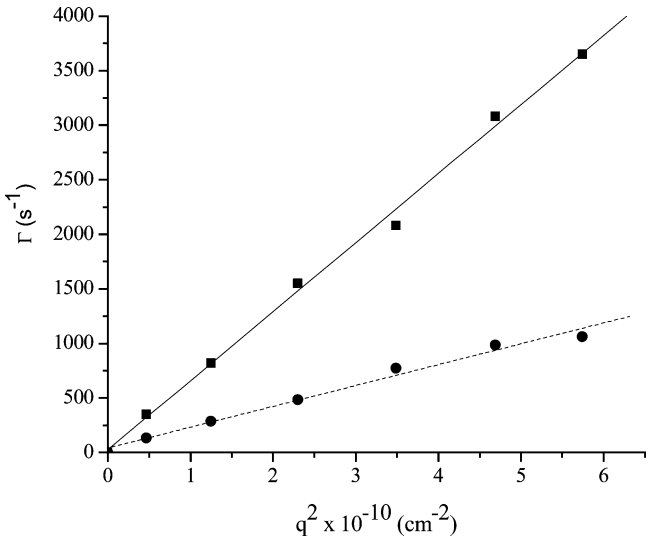

Figure 7. Dependence of the decay rate on the scattering vector for (−−) CSSQ-PEO unassociated unimolecular micelles and (- - -) micellar aggregates of CSSQ-PEO. (Concentration of CSSQ-PEO: 0.5 mg/mL).

between the micellar aggregates through the long chain PEO segments, which represents values of R_h between 100 and 150 nm. These interconnections of micellar aggregates can also be observed in the TEM micrograph.

Figure 7 shows the dependence of the decay rate (Γ) on the square of the scattering vector q [$q^2 = (4\pi n/\lambda_0 \sin \theta/2)^2$] for the unassociated unimolecular micelle and the micellar aggregates of CSSQ-PEO concentration at 0.5 mg/mL. Measurements were carried out at angles between 30 and 130°. Both peaks (as seen in Figure 6) are shown to be diffusive from the linear dependence of the decay rate passing through the intercept (0,0). The diffusion coefficients, determined from the slopes of the linear plots, are used to calculate the apparent hydrodynamic

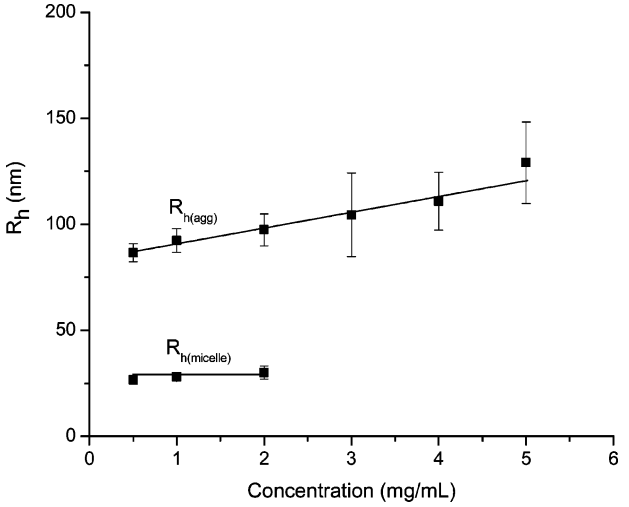

Figure 8. The concentration dependence of the hydrodynamic radii (R_h) for unassociated unimolecular micelles ($R_{h,micelle}$) and micellar aggregate ($R_{h,agg}$) of CSSQ-PEO in aqueous solution at 25 °C.

radii, R_h, of unassociated unimolecular micelles and micellar aggregate size, respectively, through the Stokes−Einstein relationship.

Figure 8 shows the concentration dependence of R_h for both unassociated unimolecular micelles ($R_{h,micelle}$) and micellar aggregates ($R_{h,agg}$) of CSSQ-PEO in aqueous solution. DLS measurements indicate that the R_h of unassociated unimolecular micelles does not depend on the concentration, while the aggregation size increases with increasing concentration. Because of the hydration of PEO segments in the outer layer, the size of CSSQ-PEO in water is large. Addition of CSSQ-PEO leads to the dehydration of PEO segments, and the intermicellar association becomes more favorable. Therefore, the dimensions of the CSSQ-PEO micellar aggregates are larger at higher concentration as indicated in Figure 8. By extrapolating to zero concentration, the R_h values for CSSQ-PEO unassociated unimolecular micelles and micellar aggregates at infinitely dilute solution are found to be 26 and 79 nm, respectively. The end-to-end distance of PEO with the size of the CSSQ cage was calculated according to the literature assuming a helical configuration of PEO[26] and found to be ~14 nm. The value of R_h for CSSQ-PEO unassociated unimolecular micelles is approximately two times larger than the end-to-end distance of CSSQ-PEO. It is not surprising that the end-to-end distance is theoretically calculated in a dry state, while DLS gives the R_h of CSSQ-PEO in aqueous solution.

The apparent molecular weight of CSSQ-PEO micellar aggregates, together with the radius of gyration (R_g) and the second virial coefficient (A_2), are determined by a Zimm plot within the concentration range of 0.5−2.0 mg/mL. The apparent molecular weight of CSSQ-PEO is found to be 4.97×10^5, which is larger than the value obtained by GPC ($M_w = 12\,950$), confirming the presence of CSSQ-PEO aggregates in water. Table 1 summarizes the fluorescence and static and dynamic light scattering results for CSSQ-PEO in aqueous solution. The large size of R_g (115 nm) also substantiates the presence of large aggregates in the solution. Note that R_g is only obtained for micellar aggregates because static light scattering cannot be used for the unassociated unimolecular micelles. The aggregation number (N_{agg}) is an important parameter to describe the characteristic of the micelle. From the apparent weight average molecular weight of CSSQ-PEO determined by static light scattering and that of molecular weight obtained by GPC, it is possible to calculate the average aggregation number of micelles in each aggregate:

$$N_{agg} = \frac{M_{w,agg}}{M_w^0} \tag{4}$$

where N_{agg} is the average aggregation number, $M_{w,agg}$ is the weight average molecular weight of CSSQ-PEO aggregates in aqueous solution, and M_w^0 is the weight average molecular weight of CSSQ-PEO determined by GPC. The N_{agg} value of CSSQ-PEO in aqueous solution is calculated to be 38, which is smaller compared to the aggregation numbers of 50 for C_{60} end-capped poly(ethylene oxide)[27] and 1020 for two-arm fullerene-containing poly(ethylene oxide).[28] This may be due to the much larger hydrophobicity of C_{60} end-capped PEO and fullerene-containing PEO compared with that of CSSQ-PEO. The N_{agg} of micelles in aqueous media increase with increase in the size and the length of hydrophobic group and decrease with increase in the cross-sectional area of the hydrophilic group.[29] In the CSSQ-PEO micelle, the size of the hydrophobic core is smaller relative to the corona area of hydrophilic PEO (shown in TEM micrograph) that may also lead to the decrease in the aggregation number.

The dimensionless parameter ρ (the ratio of R_g/R_h) can be used to determine the conformation of the polymer structure. The ρ values for the hard sphere[22,30] and star polymer with many arms[31] were reported to be 0.78 and 1.08, respectively. The value of ρ increases with decreasing number of arms in star polymers because the micelles having fewer chains exhibit a single chain behavior.[32] In this work, the ρ value is determined to be 1.46, suggesting greater thermodynamic penetrability in the outer layer of the CSSQ-PEO aggregates than in hard spheres. A large value of ρ (1.46) for CSSQ-PEO corresponds to a relatively small CSSQ core surrounded by an extremely loose shell of long chain PEOs where the solvent can drain inside more deeply. However, it should be emphasized that the magnitude of ρ also depends on polydispersity. An increase in polydispersity causes an increase in the value of ρ.[22] Baumann and co-workers[33] described the ρ value for core−shell structures of polyorganosiloxanes in the presence of cationic surfactant benzethonium chloride in different solvent systems, and their studies showed that the value of ρ depends on the quality of the solvent. The value of $\rho = 1.33$ indicates a starlike structure in a good solvent, deviating from the theoretical value of $\rho = 1.2$ for a monodisperse, starlike structure in a Θ solvent[34] with high branching density. Knischka et al.[15] reported that the values of R_g and R_h were found to be 105−115 and 60 nm for silsesquioxane-based amphiphiles, which are smaller than those values obtained in this work. The difference is that the higher molecular weight of PEO ($M_n = 2000$) was used in this study relative to the previous report ($M_n = 750$). Although the values of R_g and R_h are smaller compared to our work, the ratio of R_g/R_h is larger ($\rho = 1.75-1.9$).

The average chain density (ρ_d) of CSSQ-PEO was found to be 4×10^{-4} g cm^{-3}, calculated from the values of $M_{w,agg}$ and $R_{h,agg}$ as shown in the following equation.

$$\rho_d = \frac{3M_{w,agg}}{4\pi N_A R_{h,agg}^3} \tag{5}$$

A small value of ρ_d reveals the open coronal structure of CSSQ-PEO with a large hydrodynamic volume. Wu and coworkers[35] described that the average chain density of poly(ethylene glycol-*b*-sebacic anhydride) diblock copolymer ($\rho_d =$

TABLE 1: Fluorescence, Static and Dynamic Light Scattering Studies of CSSQ-PEO in Water at 25 °C

CAC (mg/mL)	$M_{w,agg}$ (g/mol)	R_g (nm)	R_h (nm)	R_g/R_h	A_2 (mol cm^3/g^2)	N_{agg}	ρ_d (g/cm^3)
0.27	$4.97 \pm 2.5 \times 10^5$	115 ± 2.9	79 ± 3.4	1.46	$5.6 \pm 2.8 \times 10^{-4}$	38 ± 2	4×10^{-4}

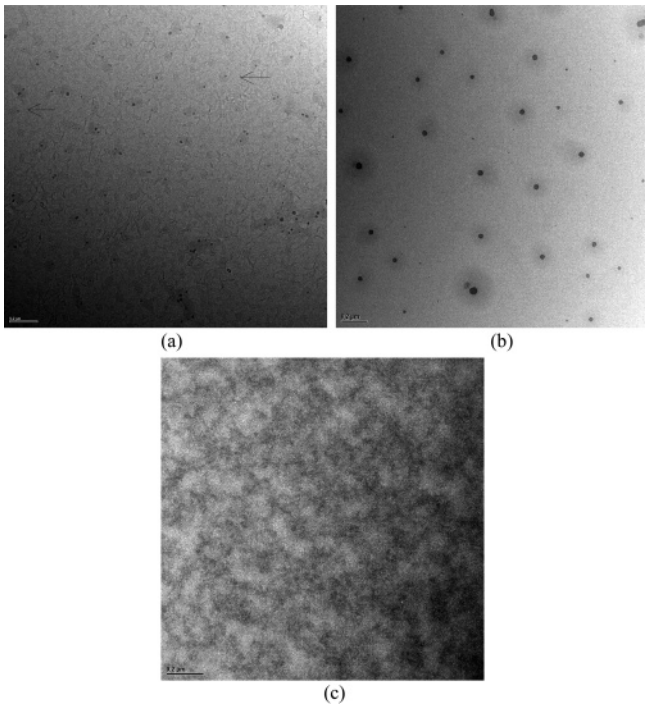

Figure 9. Transmission electron micrographs of CSSQ-PEO at different concentrations: (a) 0.25 mg/mL, (b) 1.0 mg/mL, and (c) 5.0 mg/mL. (Scale bar: 200 nm).

0.031 g/cm^3) is much lower than that of bulk polymer (~1.0 g/cm^3). It has been explained that the diblock copolymer loosely aggregates and includes a lot of water in its hydrodynamic volume. Because of the small hydrophobic core surrounded by the stretching out of the swollen PEO segments in the corona and the large penetration of water into the open structure of the micelle, the average chain density of CSSQ-PEO nanostructure is extremely small.

Figure 9 shows the TEM micrographs of CSSQ-PEO at three different concentrations. At low concentration (0.25 mg/mL, C ≤ CAC), unassociated unimolecular micelles are formed. It is pointed out that unassociated unimolecular micelles are not the usual polymeric micelles but contain the CSSQ inorganic core. The particle size obtained from TEM micrograph (Figure 9a) is in the range of 20−50 nm (the particle radius = 10−25 nm), which are somewhat smaller than those obtained by DLS (R_h = 26 nm) because TEM micrographs show the micelle with the corona shrinkage after evaporation of water, while DLS gives the size of swollen nanoparticles in aqueous solution. However, the particle radius (10−25 nm) obtained from TEM micrograph is well consistent with the calculation of end-to-end distance of CSSQ-PEO (~14 nm). At medium concentration (1.0 mg/mL, C > CAC), the isolated larger coronal micelles are observed (Figure 9b), coexisting with unassociated unimolecular micelles. In the TEM micrograph, the accumulation of hydrophobic CSSQ is represented as the dark domains that are surrounded by the PEO coronae. On the basis of the TEM micrograph, the aggregation size of the CSSQ core and the thickness of the corona can be estimated. The average diameter of the hydrophobic cores (dark domains in Figure 9b) is in the range of 46−60 nm, and the diameter of individual CSSQ nanoparticle is approximately 1.5 nm.[36,37] Therefore, the estimated aggregation number of CSSQ is 31−40, which is in good agreement with the result determined by static light scattering (N_{agg} = 38 ± 2). The average thickness of the corona layer in CSSQ-PEO aggregates is measured at 75−110 nm in the TEM micrograph. It is found that the thickness of the corona greatly exceeds the diameter of the hydrophobic core. This result confirms the structure of the small hydrophobic core surrounded by the long coronal PEO chains. At high concentration (5.0 mg/mL, C ≫ CAC), network-like aggregates are observed (Figure 9c). The formation of network structures for the modified PEO in aqueous solution has been reported.[27,38] The long PEO segments act as a spacer between the spherical aggregates, which lead to the formation of network-like aggregates at high concentration. This finding reflects the appearance of the broad distribution in DLS. Knischka et al.[15] reported that the aggregation of amphiphile leads to micellar and vesicle structures that can be cross-linked to liposome-like silica particles at elevated pH. The CSSQ-PEO micelles show spherical aggregates and do not appear to be liposome-like structures. The difference may be attributed to the different number of substituting groups and the length of PEO, which might control the structure of the aggregates.

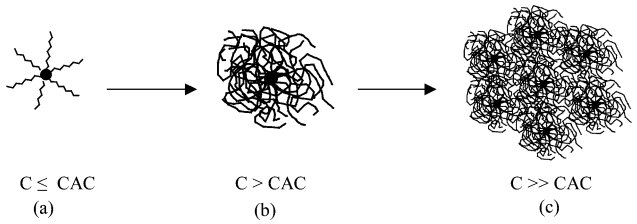

Figure 10. Schematic representation of CSSQ-PEO aggregates formation at different concentrations. (a) C ≤ CAC, (b) C > CAC, and (c) C ≫ CAC.

On the basis of the light scattering and TEM results, the conformations of the aggregates at different concentrations can be schematically illustrated as shown in Figure 10. At concentrations below CAC, there exists the unassociated unimolecular micelle consisting of a small hydrophobic CSSQ core and a corona of long-chain PEO segments, illustrated as a starlike micelle (Figure 10a). Micellar aggregation is observed with increasing CSSQ-PEO concentration (Figure 10b). Further increase in CSSQ-PEO concentration produces the stronger micellar association, leading to the formation of network-like aggregation as shown in Figure 10c.

Conclusions

Amphiphilic CSSQ-PEO was prepared and its aggregation properties in aqueous solution were investigated by fluorescence, light scattering, and TEM. A core−corona structure of unimolecular and aggregated CSSQ-PEO was found in aqueous solution. The critical aggregation concentration was determined at 0.28 mg/mL using fluorescence measurements. DLS measurements and TEM micrographs showed that unassociated unimolecular micelles coexisted with micellar aggregates at certain concentrations. The corona PEO segments were expanded and swollen in aqueous solution that may cause the CSSQ-PEO unimolecular micelles to form large-size spherical aggregates. The aggregation number (N_{agg}) of CSSQ-PEO in aqueous solution was found to be 38 ± 2, determined by SLS, which is in good agreement with the value obtained by TEM

studies. The interconnections between the micellar aggregates lead to the formation of network-like structures at higher concentration. The effect of temperature on the structure of CSSQ-PEO and its application in drug delivery systems are presently under investigation.

Acknowledgment. We gratefully acknowledge financial support from the Institute of Materials Research and Engineering (IMRE) under the Agency for Science, Technology, and Research (ASTAR).

References and Notes

(1) Feher, F. J. Wyndham, K. D.; Soulivong, D.; Nguyen, F. *J. Chem. Soc., Dalton Trans*. **1999**, 1491.
(2) Cassagneau, T.; Caruso, F. *J. Am. Chem. Soc*. **2002**, *124*, 8172.
(3) Dvornic, P. R.; Hartmann-Thompson, C.; Keinath, S. E.; Hill, E. J. *Macromolecules* **2004**, *37*, 7818.
(4) He, C.; Yang, X.; Huang, J.; Ling, T. T.; Mya, K. Y.; Zhang, X. *J. Am. Chem. Soc*. **2004**, *126*, 7792.
(5) Laine, R. M.; Choi, J.; Lee, I. *Adv. Mater*. **2001**, *13*, 800.
(6) Choi, J.; Haecup, J.; Yee, A. F.; Zhu, Q.; Laine, R. M. *J. Am. Chem. Soc*. **2001**, *123*, 11420.
(7) Lin, W. J.; Chen, W. C.; Wu, W. C.; Niu, Y. H.; Jen, A. K. Y. *Macromolecules* **2004**, *37*, 2335.
(8) Mya, K. Y.; He, C.; Huang, J.; Yang, X.; Jie, D.; Siow, Y. P. *J. Polym. Sci., Part A: Polym. Chem*. **2004**, *42*, 3490.
(9) Lichtenhan, J. D.; Schwab, J. J.; Reinerth, W. A., Sr. *Chem. Innovation* **2001**, *1*, 3.
(10) Cheng, H.; Tamaki, R.; Laine, R. M.; Babonneau, F.; Chujo, Y.; Treadwell, D. R. *J. Am. Chem. Soc.* **2000**, *122*, 10063.
(11) Zhang, C.; Laine, R. M. *J. Am. Chem. Soc.* **2000**, *122*, 6979.
(12) Lamm, M. H.; Chen, T.; Glotzer, S. C. *Nano Lett.* **2003**, *3*, 989.
(13) Kim, B.-S.; Mather, P. T. *Macromolecules* **2002**, *35*, 8378.
(14) Maitra, P.; Wunder, S. L. *Chem. Mater*. **2002**, *14*, 4494.
(15) Knischka, R.; Dietsche, F.; Hanselmann, R.; Frey, H.; Mullhaupt, R. *Langmuir* **1999**, *15*, 4752.
(16) Winnik, M. A.; Yekta, A. *Curr. Opin. Colloid Interface Sci*. **1997**, *2*, 424.
(17) Lee, A.; Xiao, J.; Feher, F. J. *Macromolecules* **2005**, *38*, 438-444.
(18) Huglin, M. B. *Light Scattering from Polymer Solutions*; Academic Press: London, 1972; p 90.
(19) Lestel, L.; Cheradame, H.; Boileau, S. *Polymer* **1990**, *31*, 1154.
(20) Hasegawa, I.; Motojima, S. *J. Organomet. Chem*. **1992**, *441*, 373.
(21) Gravel, M. C.; Zhang, C.; Dinderman, M.; Laine, R. M. *Appl. Organomet. Chem*. **1999**, *13*, 329.
(22) Brown, W. *Laser Light Scattering, Principles and Developments*; Clarendon Press: Oxford, 1996.
(23) Li, J.; Li, X.; Ni, X.; Leong, K. W. *Macromolecules* **2003**, *36*, 2662.
(24) Bailey, J. L.; Koleske, J. V. *Poly(Ethylene Oxide)*; Academic Press: New York, 1976.
(25) Narrainen, A. P.; Pascual, S.; Haddleton, D. M. *J. Polym. Sci., Part A: Polym. Chem*. **2002**, *40*, 439.
(26) Johnson, J. A.; Saboungi, M. L.; Price, D. L.; Ansell, S. *J. Chem. Phys*. **1998**, *109*, 7005.
(27) Song, T.; Dai, S.; Tam, K. C.; Lee, S. Y.; Goh, S. H. *Langmuir* **2003**, *19*, 4798.
(28) Song, T.; Dai, S.; Tam, K. C.; Lee, S. Y.; Goh, S. H. *Polymer* **2003**, *44*, 2529.
(29) Rosen, M. J. *Surfactants and Interfacial Phenomena*, 2nd ed.; John Wiley & Sons: New York, 1988; p 114.
(30) Pike, E. R.; Abbiss, J. B. *Light Scattering and Photon Correlation Spectroscopy*; Kluwer Academic Publishers: Netherlands, 1996; p 178.
(31) Burchard, W.; Schmidt, M.; Stockmayer, W. H. *Macromolecules* **1980**, *13*, 1265.
(32) Vagberg, L. J. M.; Cogan, K. A.; Gast, A. P. *Macromolecules* **1991**, *24*, 1670.
(33) Baumann, F.; Schmidt, M.; Weis, J.; Deubzer, B.; Geck, M. Dauth, J. Core Shell Structures Based on Polyorgano Silicone Micronetworks Prepared in Emulsion. In *Organosilicon Chemistry II: From Molecules to Materials*, Auner, N., Weis, J., Eds.: Weinheim: New York, 1996; p 670.
(34) Schmidt, M. In *Dynamic Light Scattering: Applications to Structures Analysis* Brown, W., Ed.; Oxford University Press: Oxford, 1993; p 372.
(35) Wu, C.; Fu, J.; Zhao, Y. *Macromolecules* **2000**, *33*, 9040.
(36) Choi, J.; Yee, A. F.; Laine, R. M. *Macromolecules* **2003**, *36*, 5666.
(37) Zheng, L.; Waddon, A. J.; Farris, R. J.; Coughlin, E. B. *Macromolecules* **2002**, *35*, 2375.
(38) Zhang, K.; Xu, B.; Winnik, M. A.; MacDonald, P. M. *J. Phys. Chem*. **1996**, *100*, 9834.